Journal of Computer-Aided Molecular Design, 4 (1990) 355–367
ESCOM



J-CAMD 094

# Molecular modeling studies on the urease active site and the enzyme-catalyzed urea hydrolysis

Ramiro Medina[a,*] and Klaus Müller[b]

[a]*Lehrstuhl für Allgemeine Chemie und Biochemie der TU München, W-8050 Freising-Weihenstephan, Germany*
[b]*Central Research Units, F. Hoffmann-La Roche Ltd., CH-4002 Basel, Switzerland*

Received 16 February 1990
Accepted 23 March 1990

*Key words:* Urease active site; Substrates; Inhibitors; Molecular modeling; Urea hydrolysis

## SUMMARY

These studies are an attempt to gain better insight into the pharmacophore requirements of urease. On the basis of published information on this enzyme (EXAFS, amino acid sequence, essential groups at the active site) a hypothetical nickel-tripeptide complex, as preliminary substitute for the urease active site was modeled using computer-aided molecular modeling techniques. The results suggest two alternative docking modes of urea and reaction intermediates, corresponding to two different reaction mechanisms. Both binding modes are compatible with the docking of known potent inhibitors such as selected hydroxamic acids and phosphorodiamides. The results can be used to help in the design of new potential inhibitors of urease.

## INTRODUCTION

The basic food for two-thirds of the world's population is rice, which in 1985 accounted for slightly more than 25% of the world's cereal production [1].

At present, urea is the most available and frequently used nitrogen fertilizer on rice [2]. However, when urea is applied to flooded rice fields, the efficiency of nitrogen utilization is usually low, only 30–40% [3]. There are several loss mechanisms that cause this low efficiency: ammonia volatilization, nitrification, denitrification, runoff, and leaching [4]. Among these, ammonia volatilization is probably the most significant and is directly related to the hydrolysis of urea catalyzed by urease [5]. Urease is an enzyme that is present in soils. Control of the rate of ammonia formed by urea hydrolysis in rice paddies should lead to improved nitrogen use efficiency. One way to reduce this ammonia volatilization is to add certain compounds to the soils along with urea that would inhibit urease activity, thereby retarding urea hydrolysis [6].

Urea is hydrolyzed by urease to ammonium ion and carbamate, which decomposes to carbon

* To whom correspondence should be addressed.

dioxide and ammonia. Essential groups of the active site have been identified as two coordinated nickel ions, a thiol group, a negatively charged carboxylate ion [7], and an imidazole group [8].

Two mechanisms of urea hydrolysis by urease have been proposed [9, 10]. The tertiary structure of the urease is still unknown and only indirect methods have been applied to map the active site of this enzyme. Kobashi and co-workers [11–13] have used quantitative structure-activity relationships to correlate urease inhibitory potencies and structures of hydroxamic acids based partly on quantum chemistry calculations. Recently, using urease substrates and inhibitors, a pharmacophore model was derived, which included approximate dimensions of the active site and three areas sensitive to steric hindrance [14].

For a more precise conception of urease inhibitors with optimal chemical structures for interaction with the enzyme cavity, more information is necessary about the spatial arrangement of essential groups, hydrophobic pockets, and the specific chemical environment surrounding the nickel atoms at the active site. Alagna et al. [15] reported the results of an extended X-ray absorption fine structure analysis (EXAFS) of the Jack Bean urease active center and compared it to model structures. Their results indicated that the nickel ions in urease are bound in part to imidazolyl groups, forming a quasi-octahedral complex together with some other nitrogen- or oxygen-containing ligands. Mamiya et al. [16] determined and reported the complete amino acid sequence of Jack Bean urease and recognized $Cys^{592}$ as essential for enzymatic activity. Additionally, this cysteine is followed by two histidine residues in the sequence Cys-His-His. On the basis of this information and assuming that this tripeptide is involved in the complexation of a nickel ion at the active site, we modeled a hypothetical cavity of the enzyme and its potential interactions with selected substrates and inhibitors, in an attempt to gain better insight into the pharmacophore requirements of this enzyme.

## METHODS

Modeling was performed using the Roche Interactive Molecular Graphics RIMG [17] software package developed at Hoffmann-La Roche, Basel, running on a DEC VAX-11/780 computer connected to an Evans & Sutherland Color Multi-Picture System. The geometry of an octahedrally coordinated Ni(II) complex was defined with reference to seven well resolved X-ray structures of relevant Ni(II) complexes*, retrieved from the Roche Cambridge Structural Database, ROCSD [17]. Superposition of these structures using the algorithm of Gerber and Müller [25], followed by structural averaging, produced a hexacoordinated Ni(II) template that was used in the modeling and geometry optimization of octahedral Cys-His-His-$NH_2$ Ni(II) complexes**. These structures served as hypothetical models of the enzyme active site. They allowed us to dock substrate and inhibitor molecules and to probe putative reaction intermediates. Energy refinements of ligands were based on a generalized united-atom force field for organic molecules [26, 27].

---

*1. A. bis(histidino)nickel(II)monohydrate [18], 2. B. bis(L-histidinato)nickel(II)monohydrate [19], 3. C. bis(glycinato) bis(imidazole)nickel(II) [20], 4. D. aquo-*cis*-bis(histamino)-perchlorate nickel(II)perchlorate [21], 5. E. diaqua-histidinato-isothiocyanato-nickel(II)monohydrate [22], 6. F. tri-(histamine)nickel(II)perchlorate [23], 7. G. *trans*-diaqua-bis(prolinato)nickel(II) [24].

**Atomic coordinates of the Ni(II)–tripeptide model complexes can be obtained on request from the authors.

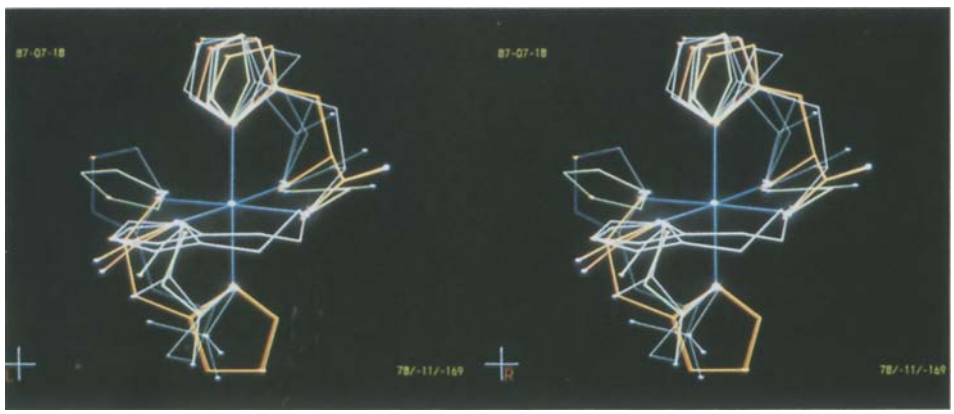

Fig. 1. Optimal least-squares superposition of hexacoordinated Ni(II) complexes (see footnote *). Averaged, symmetrized octahedral Ni(II) ligand field (blue), X-ray structures of complex A (red), B (orange), C (green), D, E, F, G (white).

## RESULTS AND DISCUSSION

The superposition of the seven hexacoordinated histidine, histamine, and imidazole Ni(II) complexes (see footnote*) is shown in Fig. 1. Some scattering of the ligand positions is observed. An averaged and symmetrized octahedral ligand field for Ni(II) is displayed in blue. This structural model represents an adequate reference for our modeling Ni(II)-complexes involving histidine or histidine-like ligands.

In a second step the model of the tripeptide Cys-His-His-$NH_2$, constructed from standard amino acid and peptide geometries, was docked to this Ni(II) ligand template in two possible binding modes, leading to the syn-(CON-syn)- and anti-arrangements (CON-anti) of the imidazole rings shown in Figs. 2A and B, respectively.

In the configurations displayed in yellow the valence angles were preserved at standard values and ligand positions match within 0.1 Å, but some deviations from optimal stereoelectronic arrangements are observed. In order to improve stereoelectronic aspects of ligand binding, pseudo-Ni atoms were attached to all relevant ligand positions assuming trigonal planar arrangements at $sp^2$-N atoms with 2.15 Å and 2.09 Å distances for (peptide)N-Ni(II) and (imidazole)N-Ni(II) bonds, respectively. The nitrogen atoms of the tripeptide were then matched to the ligand positions while forcing the four pseudo-Ni atoms to match on top of the real Ni atom. As a consequence, proper $\sigma$-binding of the $sp^2$-hybridized nitrogen atoms could be effected without major distortions of the valence geometries of the ligands (maximum valence angle deformations ca. 3–4 degrees). These two optimized configurations are also displayed in Figs. 2A and B (blue structures), respectively. Both structures of the syn-configuration are virtually strainless. The two anti-configurations exhibit some residual torsional strain as well as nonbonded repulsions around the His-His peptide linkage. Hence, the anti-arrangement seems to be less favored than the syn-configuration. In all cases the complexing N-atoms superimpose within 0.1Å on top of the ligand positions of the octahedral Ni(II) reference template.

Before proceeding, let us confront our model with known results of metal-peptide complex chemistry.

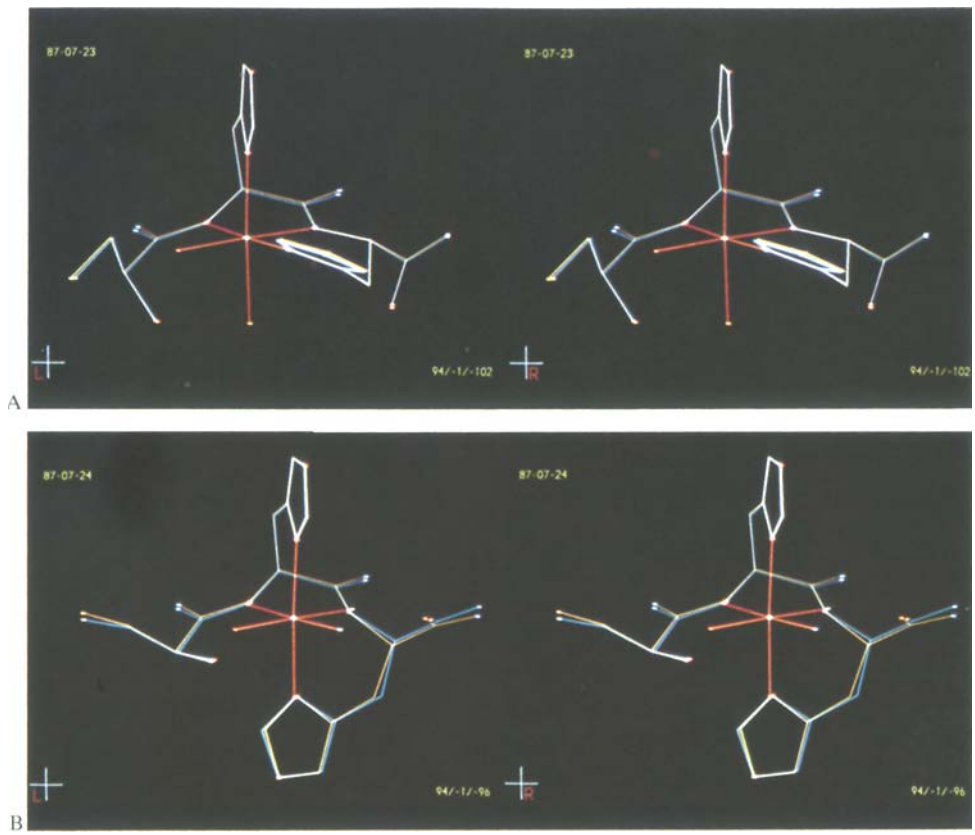


Fig. 2. Docking of the tripeptide Cys-His-His-$NH_2$ to the Ni(II) ligand field (red). (A) Syn-configuration (CON-syn), (B) anti-configuration (CON-anti).

The interactions of amino acids and peptides with transition metal ions are well documented [28, 29]. Especially the Cu(II) and Ni(II) complexes with oligopeptides have been carefully investigated [30–32]. Ionization of amide hydrogens is markedly promoted in the presence of Cu(II) or Ni(II) ions so that deprotonation can occur even at physiological pH [33]. This is especially true when a histidyl residue is involved, which can serve as an anchor for the metal ion [34]. While Cu(II) forms tetragonal complexes, Ni(II) forms complexes of two distinctly different stereochemistries, viz., blue or green octahedral complexes of paramagnetic hexacoordinated Ni(II) and yellow square planar complexes of diamagnetic tetracoordinated Ni(II). The former is observed, for instance, in the glycyl-glycine complex containing two bidentate Gly-Gly ligands chelated via the amino and deprotonated amide nitrogens and a carboxylate oxygen [31]. By contrast, with glycinamide, triglycine, tetraglycine, histidylhistidine, and higher peptides, transitions from paramagnetic octahedral to diamagnetic square-planar complexes are observed [34]. These transitions are related to the deprotonation of two or more peptide nitrogens, resulting in a spin pairing into a planar complex [34]. Margerum and co-workers [35, 36] studied the effect of coordinated ligands on the rate of exchange of bound water by ammonia in Ni(II) complexes. They concluded that the

multidentate ligands complexed to nickel are not displaced in the reaction and that exchange rates for coordinated water are influenced by the number of coordinated nitrogens in nickel-polyamine complexes. Thus, an increase in the number of coordinated nitrogen ligands tends to accelerate the replacement of the remaining coordinated water molecules. Six-membered chelate rings in polyamine complexes also increase the water exchange rate.

In both the syn- and anti-forms of our Ni-peptide model, the peptide chelates nickel as a quadridentate ligand with four nitrogen donor atoms, two deprotonated peptide nitrogens with Ni-N bond lengths of 2.15 Å and two imidazole pyridine nitrogens with Ni-N bond lengths of 2.09 Å. The two additional ligands, which complete the Ni hexacoordination sphere, are water molecules with Ni-O bond lengths of 2.15 Å. All these bond distances agree within 0.1 Å with the corresponding bond lengths reported by Alagna et al. [15] based on EXAFS measurements on crystalline urease. From their results and by comparison with model compounds, the authors have concluded that the nickel ion coordinates to histidyl groups and that the first coordination sphere of the nickel ion is composed of some combination of only nitrogen and oxygen donors. Furthermore, the absorption spectrum of the urease does not display the characteristic $RS^-$ Ni(II) charge transfer transitions normally found in simple thiolate Ni(II) complexes or in Ni(II)-proteins containing one, two or four $RS^-$ ligands [37].

Accordingly, in our model we propose a combination of four nitrogen and two oxygen atoms as donors and we do not consider the cysteinyl group as a nickel ligand.

In agreement with histidylhistidine-Ni(II) complex chemistry, we propose binding of Ni(II) by deprotonation of two peptide units, so that a complex of optimal configuration with four probably very stable and strainless chelate rings (see Fig. 3) can be formed. By such a quadridentate chelation, which still leaves two ligand positions for catalytic activity, the nickel ion is tightly bound and considerably shielded. This conforms to the finding that Jack Bean urease is stable and fully active in the presence of dimethylgloxime at all the stages of purification [38] and also in the presence of EDTA at neutral pH [39, 40]. At lower pH (3.5–4.0) EDTA appears to promote the loss of Ni(II) and the irreversible inactivation of urease [38].

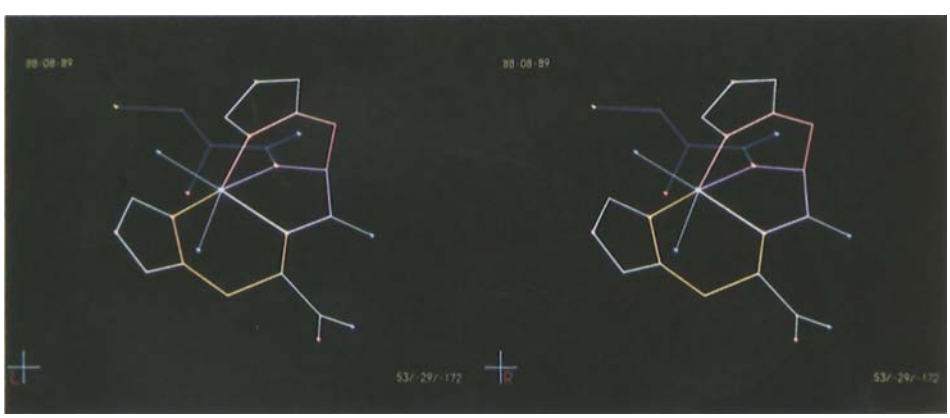

Fig. 3. The cysteinylhistidylhistidine hexacoordinate-Ni(II) complex (CON-syn) as a model for the active site of the urease. The strainless complex contains a five-, a seven-, and two six-membered chelate rings, which are highlighted in purple, pink, and yellow, respectively.

There is one apparent inconsistency between our model and the known chemistry of Ni-peptide complexes. With two or more deprotonated peptide units, such complexes normally undergo spin pairing and adopt planar tetracoordinated forms. This is in conflict with our proposed octahedral structure of a cysteinylhistidylhistidine-Ni(II) complex. Here, we have to resort to the entatic state hypothesis [41], which states that specific protein environments may hold transition metal ions in unusual ligand geometries and/or electronic states thereby enhancing their potential catalytic activities. In this respect, it is of interest to remember that Zn(II) or Co(II) bind to carboxypeptidase A with rather unusual pentacoordinated complex geometries. When Zn(II) is replaced by Ni(II), the nickel ion moves with its bound water molecule by about 0.5 Å to engage in an octahedral-minus-one complex, with the sixth ligand position unoccupied [42].

In the absence of further chemical and structural information on urease, we may use our Ni-peptide models as preliminary substitutes for the real enzyme active site to dock substrates and inhibitor molecules and to probe putative reaction intermediates. Clearly, our proposed Ni-peptide model for the urease active site remains highly speculative. Further chemical and structural information on urease is necessary to refine or modify our preliminary model. Nevertheless, this model may be useful to aid in urease inhibitor design. As an illustration, we have used this model to dock substrate and inhibitor molecules and to probe putative reaction intermediates.

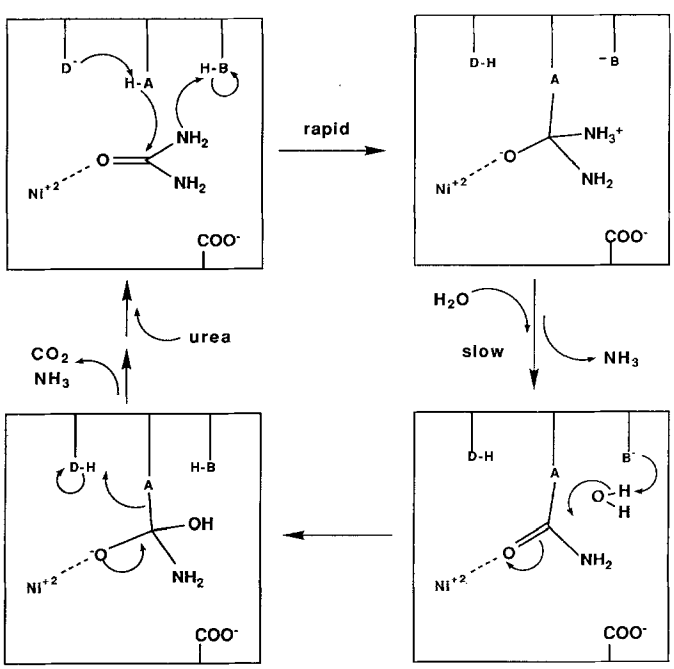


Fig. 4. Active site of urease and proposed mechanism of urea hydrolysis. In mechanism 1, AH is a thiol group, -SH, in mechanism 2, AH is a Ni(II)-coordinated hydroxide ion, Ni-OH. The group represented by -BH corresponds to a histidine unit in mechanism 1 and a thiol group in mechanism 2. D represents a base.

## REACTION MECHANISMS OF THE UREASE AND DOCKING OF UREA

As indicated above, essential groups of the urease have been identified as two coordinated nickel ions, a thiol group, a negatively charged carboxylate ion and a histidine unit, which is not involved in the Ni(II) chelation. Two mechanisms of the urease hydrolysis of urea have been proposed [9, 10]. The basic steps of the two mechanisms are schematically represented in Fig. 4.

In both mechanisms it is assumed that substrate activation occurs through Ni complexation at the carbonyl oxygen atom and that binding of urea is further stabilized by a favorable interaction between one urea $NH_2$ unit and a nearby carboxylate group. A tetrahedral intermediate is formed by the attack of the thiol group (mechanism 1) or of the nickel coordinated hydroxide ion (mechanism 2) to the carbonyl carbon. The breakdown of the tetrahedral intermediate to form a carbamoyl-urease complex intermediate and ammonia is facilitated by a histidine residue (mechanism 1) or by a thiol group of the cysteine side chain (mechanism 2), both acting as general acid catalysts. The breakdown of the tetrahedral intermediate is the rate-limiting step [9], followed by a ra-

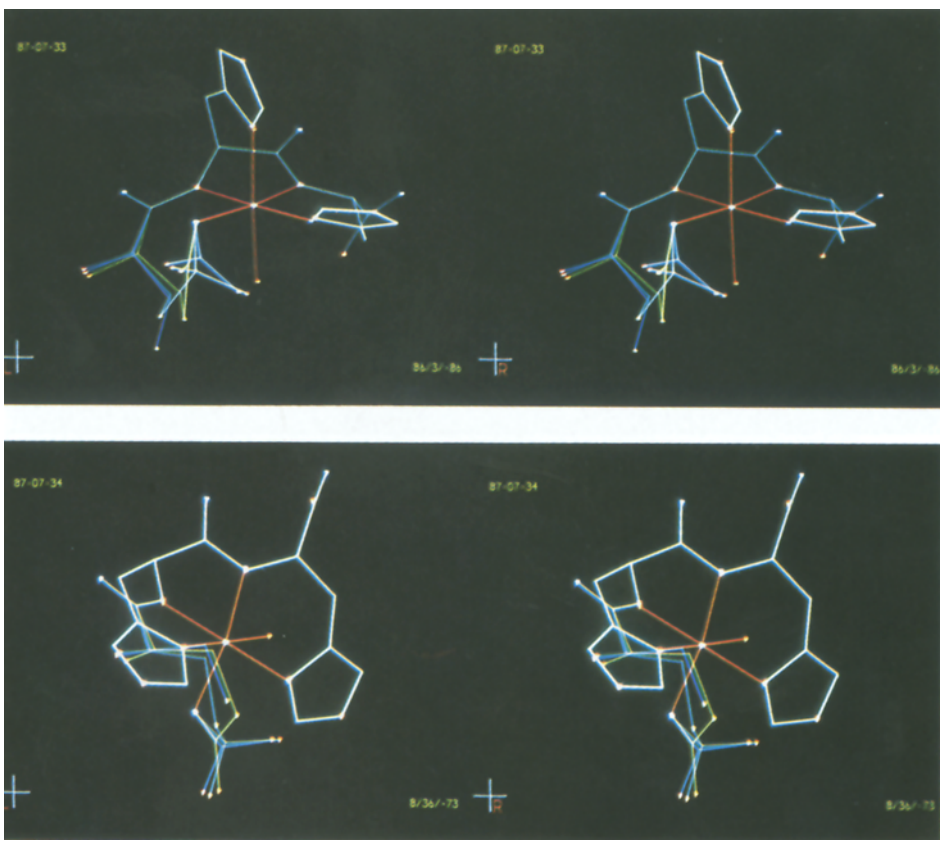

Fig. 5. Superposition of three hypothetical stages of the urea hydrolysis along the reaction path of mechanism 1 based on the active site model CON-syn. (A) Side view, trigonal urea (blue) tetrahedral intermediate (cyan), trigonal thiocarbamate intermediate (green), (B) top view.

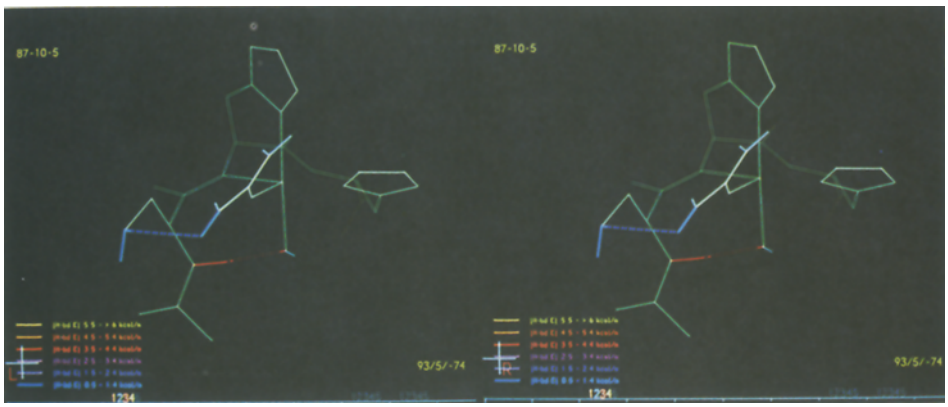

Fig. 6. Alternative docking mode of urea to the active site model CON-syn (according to mechanism 2). A weak hydrogen bond interaction between one amino group of urea and the cysteine side chain is indicated by the blue dotted line. A strong hydrogen bond between the apical $OH^-$ ligand and the backbone-NH of cysteine is shown by the red dotted line.

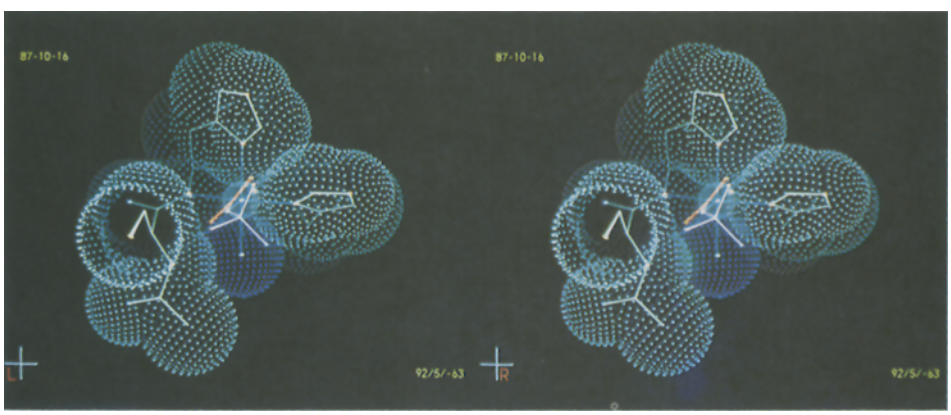

Fig. 7. Alternative docking of urea (red) and tetrahedral intermediate (violet) to the tripeptide model CON-syn (displayed with dotted van der Waals surface). The intermediate may be formed by a nucleophilic attack of the hydroxyl ion ligand (blue) to the carbonyl carbon of urea (mechanism 2).

pid hydrolysis of the carbamoyl-urease complex, liberating ammonia, carbon dioxide and urease.

Our exploratory studies show that in both cases the sequence of the postulated reaction intermediates could be easily modeled with the active site model CON-syn, but not with CON-anti, where docking of the substrate and appropriate juxtapositions of the Cys side chain would produce prohibitive torsional strain in the peptide backbone and/or collisions between the ligands bound to the nickel ion. Both reaction sequences with the CON-syn model will be discussed in the following.

*Mechanism 1*

Figure 5 shows the superposition of three stages along the reaction path of mechanism 1 based on the active site model CON-syn. The initial configuration is a fully relaxed structure (blue) with

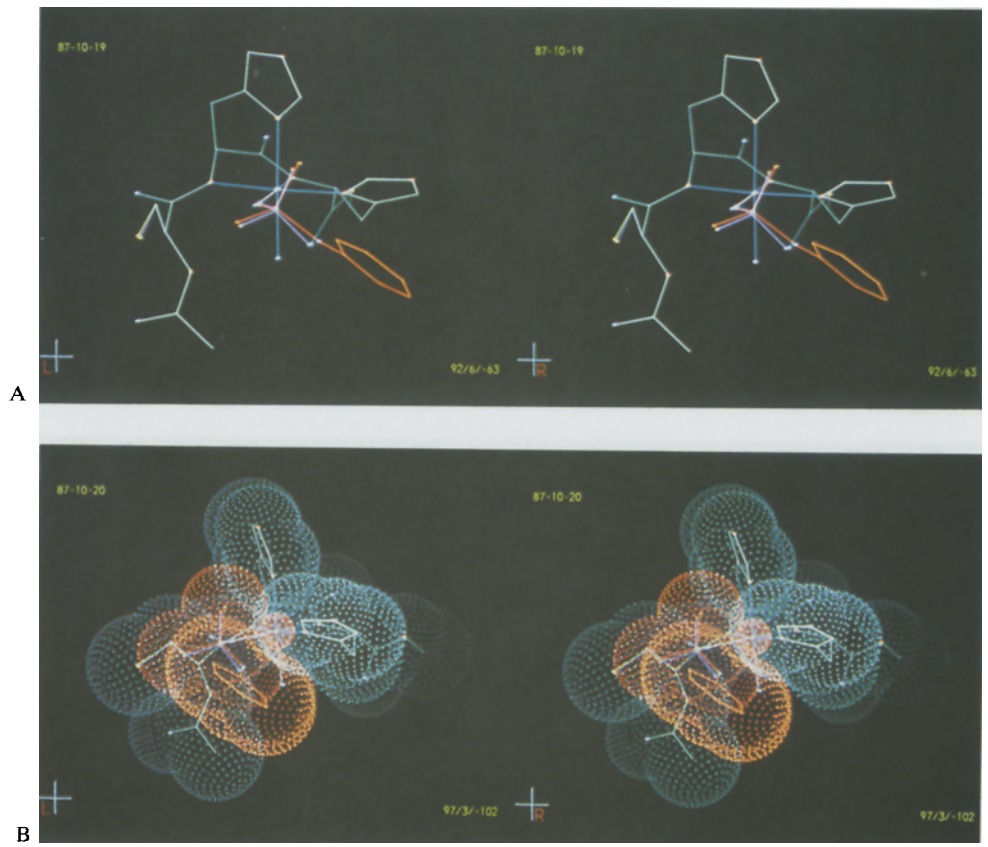


Fig. 8. (A) Docking of *O*-phenyl phosphorodiamide (red) to the active site model CON-syn (blue and cyan). The cysteine position corresponds to the binding mode of mechanism 2. The tetrahedral intermediate (violet) is also shown. (B) Similar to A with display of dotted van der Waals surface. The model is rotated about 60° for clarity. *O*-phenyl phosphorodiamide and Ni(II) ion are colored in red and CON-syn in blue.

unstrained ligands in a conserved Ni(II) coordination geometry. Note that the Cys side chain is already properly positioned for a nucleophilic attack on the urea carbonyl group. Likewise, the tetrahedral intermediate involving the thiol group (cyan) exhibits no ligand strain.

The S-C bond adopts a staggered conformation with one oxygen lone pair antiperiplanar to one scissile C-N bond. Note that the positions of the two urea nitrogen atoms remain essentially unaffected by this nucleophilic attack so that any stabilizing interaction with the remaining enzyme cavity (e.g., a carboxylate group or an activated ligand bound to the second Ni(II) ion) is preserved. Cleavage of one C-N bond leads to a Ni-complexed thiocarbamate intermediate (green). Partial relaxation, keeping the His-His dipeptide unit fixed, results in an intermediate without nonbonded collisions between ligand atoms, but with some residual strain in the thiocarbamate unit due to (i) a slightly twisted thiol-ester conformation (torsion angle about the C-S bond $-11$ degrees) and (ii) a possibly suboptimal complexation of the carbonyl oxygen out of the sigma plane (torsion angle Ni-O-C-S, ca. $-45$ degrees). We are not in a position to assess the exact amount of strain, incurred by this nonplanarity. However, our result is of interest in view of

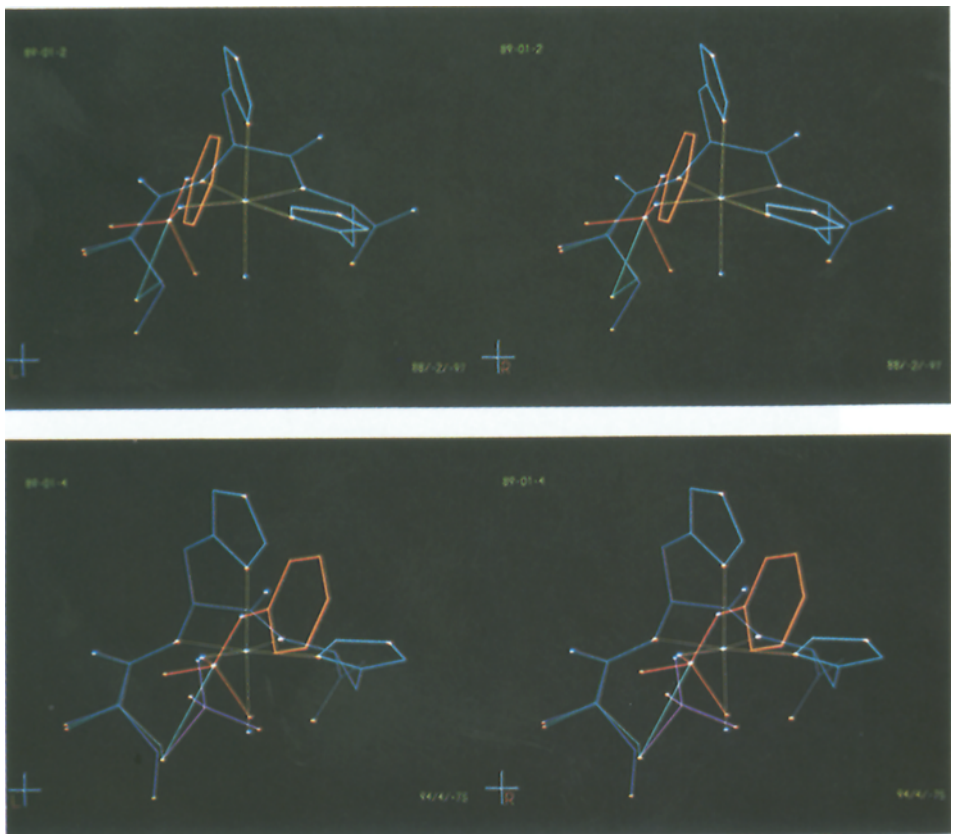

Fig. 9. (A) Docking of *O*-phenyl phosphorodiamide (red) to the CON-syn model in the binding mode of mechanism 1. The ligand structure before the nucleophilic attack is displayed in blue; After the nucleophilic attack of Cys-S to the phosphorus atom, the S-P bond (green) is oriented coaxially to the P-O (phenyl) bond axis leading to a trigonal-bipyramidal intermediate. The phenyl group shows interactions with both His side chains. (B) Similar to A with additional display of the tetrahedral intermediate of bound urea by nucleophilic attack of Cys-S to the carbonyl-carbon (violet).

the fact that the rate-limiting step in urease-catalyzed hydrolysis is the cleavage of the C-N bond in the tetrahedral intermediate [9]. As is clearly visible in Fig. 5, the transitions from the initial state to the thiocarbamate via the tetrahedral intermediate are associated with a minimum amount of structural rearrangements for both active site model and the substrate molecule.

*Mechanism 2*

An alternative docking mode of urea is shown in Fig. 6. In this orientation the carbonyl group of bound urea cannot be nucleophilically attacked by the thiol group of cysteine. However, according to mechanism 2, the closely placed thiol group may promote C-N bond cleavage by protonation of one $NH_2$ group of the tetrahedral intermediate. In order to accommodate this interaction mode, the Cys unit has to adopt a conformation in which the N-terminal peptide NH group comes into hydrogen bonding contact with an oxygen atom assumed to occupy the sixth coordination site of Ni.

As shown in Fig. 7, the urea molecule is now perpendicular to a channel formed by the Ni-complexing tripeptide so that the vector for nucleophilic attack on the carbonyl group points along the channel axis.

Note that a water molecule (or hydroxyl ion) located at the sixth coordination site could, with only minor structural adjustments of the ligand sphere, act as an intramolecular nucleophile through this channel. Alternatively, a water molecule, activated by the immediate protein environment or by the second Ni ion, could attack through this channel.

Thus, our modeling results suggest two alternative docking modes of urea to the urease active site model CON-syn, one conforming to mechanism 1, the other supporting mechanism 2. In view of the hypothetical nature of the Cys-His-His-Ni cavity and the lack of further experimental evidence, we abstain from differentiating between the two binding modes. However, both may be used to help in the design of new potential inhibitors of urease. Experimental data from specifically designed inhibitors can then be used to further refine or modify the active site model of urease and to identify the preferred binding mode.

## DOCKING OF UREASE INHIBITORS

Among the many known inhibitors of urease, the two most potent belong to two major chemical classes, i.e., phosphorodiamides and phosphorotriamides, and hydroxamic acid derivatives. Assuming that phosphorodiamides and hydroxamic acids act as mono- and bidentate Ni-ligands, respectively, we examined the complexation of typical representatives of each class in either binding mode to the hypothetical Ni-cavity. In agreement with abundant X-ray structural information on related Fe-hydroxamate complexes, docking of simple bidentate hydroxamate ligands is straightforward and dictated mainly by the location of the two water coordination sites at Ni. Little information is expected to be gained about possible binding modes of urea from such inhibitors, because the active site models for the two potential binding modes differ only in the conformation of the Cys unit, both being compatible with the complexation of a bidentate ligand.

By contrast, docking of monodentate tetrahedral phosphorodiamide derivatives may provide more information, because of their analogy to the tetrahedral intermediate of the urea hydrolysis.

Thus, a model of *O*-phenyl phosphorodiamide was docked to the same coordination site that was occupied by urea and freely relaxed to minimize steric interactions with the peptide of the active site model. Using the structural information of the two hypothetical models for the two tetrahedral intermediates, several orientations of the phosphorodiamide unit were explored. For the binding mode of mechanism 2, an almost perfect and strainless fit was obtained, with the phenoxy unit lying in the channel for a potential attacking nucleophile, and the two amide groups superimposing on top of the two amine units of the tetrahedral intermediate (Fig. 8).

For the binding mode of mechanism 1, an orthogonal placement of the *O*-phenyl phosphorodiamide is obtained, in which the phenoxy group is in tight contact with both histidine side chains (Fig. 9) and the two amide groups are situated approximately at the locations of the two nitrogen atoms of the tetrahedral intermediate.

Interestingly, the tetrahedral arrangements of the intermediates derived from the substrate or from the inhibitor differ characteristically. In the case of the substrate intermediate, the tetrahedral C atom is below the plane defined by the oxygen and the two nitrogen atoms, because it is involved in a C-S bond to Cys after nucleophilic attack. In the case of the phosphorodiamide, the

P atom is above the plane of the oxygen and nitrogen atoms, leaving a potential fifth coordination site of phosphorus available to the nucleophilic thiol group. The addition of this nucleophilic group leads to a pentacovalent trigonal-bipyramidal intermediate in the transition state of the reaction, in accordance with the assumed role of the thiol group in mechanism 1. Our results suggest, that the enzymatic hydrolysis of *O*-phenyl phosphorodiamide to phosphoric acid diamide and phenol [43], follows an associative in-line mechanism, in which the attacking nucleophile enters from the opposite side of the leaving group.

## CONCLUSIONS

In Fig. 3, we propose a cysteinylhistidylhistidine-Ni(II) complex (CON-syn) as a model for the active site of the urease. CON-syn is virtually strainless and chelates the nickel ion very tightly as a quadridentate ligand. The Ni-N and Ni-O bond lengths involving the tripeptide and the two water molecules agree within 0.1 Å with the corresponding bond lengths of the EXAFS measurements on crystalline urease. CON-syn is consistent with the known chemistry of Ni-peptide complexes and the structural chemistry of the urease reported in the last years, except for a remaining uncertainty with respect to the preference of an octahedral over a square-planar geometry of the peptide ligand sphere.

Docking of urea (also valid for the small molecules of the other substrates, formamide, acetamide, *N*-hydroxyurea, *N*-methylurea and semicarbazide) and reaction intermediates suggest two alternative binding modes, corresponding to two proposed mechanisms of reaction (Figs. 6 and 7). Finally, these two binding modes are consistent with the docking of typical urease inhibitors: hydroxamic acid and phosphorodiamide derivatives (Figs. 8 and 9).

Further information about the protein environment at the active site of urease, complementary application of the pharmacophore method using active and inactive analogs, and additional experimental data from specifically designed inhibitors may help to further refine, modify or reject the proposed active site models and to identify the preferred binding mode.

## REFERENCES


1 Martinez, A. and Diamond, R.B., In Hauck, R.D. (Ed.) Nitrogen Use in World Crop Production, American Society of Agronomy, Madison, WI, 1985.
2 Harre, E.A. and Bridges, J.D., In Bock, B.R. and Kissel, D.E. (Eds.) Ammonia Volatilization from Urea Fertilizers: Importance of Urea Fertilizers, National Fertilizer Development Center, Tennessee Valley Authority, Muscle Shoals, AL, 1988, Bulletin Y-206, pp. 1–15.
3 Vlek, P.L.G. and Craswell, E.T., Soil Sci. Soc. Am., 43 (1979) 352.
4 Terman, G.L., Adv. Agron., 3 (1979) 189.
5 Vlek, P.L.G. and Craswell, E.T., Fertilizer Res., 2 (1981) 227.
6 Mulvaney, R.L. and Bremner, J.M., In Paul, E.A. and Ladd, T.N. (Eds.) Soil Biochemistry, Vol. 5 (Control of Urea Transformations in Soils), Marcel Dekker, Inc., New York, NY, 1981, pp. 153–196.
7 Blakeley, R.L. and Zerner, B., J. Mol. Catal., 23 (1984) 263.
8 Barth, A. and Michel, J.J., Biochem. Physiol. Planzen, 163 (1972) 103.
9 Medina, R., Olleros, T. and Schmidt, H.-L., In Schmidt, H.-L., Förstel, H. and Heinzinger, J. (Eds.) Stable Isotopes (Proceedings of the 4th International Conference), Jülich, Elsevier, Amsterdam, 1981, pp. 77–82.
10 Dixon, N.E., Riddles, P.W., Gazzola, C., Blakeley, R.L. and Zerner, B., Can. J. Biochem., 58 (1980) 1335.
11 Kumani, K., Tomioka, S., Kobashi, K. and Hase, J., Chem. Pharm. Bull., 20 (1972) 1599.
12 Munakata, K., Kobashi, K. and Hase, J., J. Pharm. Dyn., 3 (1980) 457.

13 Kanoda, M., Shinida, H., Kobashi, K., Hase, J. and Nagahara, S., J. Pharm. Dyn., 5 (1982) 49.
14 Medina, R. and Radel, R.J., In Bock, B.R. and Kissel, D.E. (Eds.) Ammonia Volatilization from Urea Fertilizers: Mechanisms of Urea Inhibition, National Fertilizer Development Center, Tennessee Valley Authority, Muscle Shoals, AL, 1988, Bulletin Y-206, pp. 137–174.
15 Alagna, L., Hasnain, S.S., Piggott, B. and Williams, D.J., Biochem. J., 220 (1984) 591.
16 Mamiya, G., Takishima, K., Masakuni, M., Kayumi, T., Ogawa, K. and Sekita, T., Proc. Japan Acad., 61 (1985) 395.
17 Müller, K., Amman, H.J., Doran, D.M., Gerber, P.R. and Schrepfer, G., in Harms, A.F. (Ed.) Innovative Approaches in Drug Research, Elsevier, Amsterdam, 1986, pp. 125–133.
18 Sakurai, T., Iwasaki, H., Katano, T. and Nakahashi, Y., Acta Crystallogr. Sect. B, 34 (1978) 660.
19 Fraser, K.A. and Harding, M.M., J. Chem. Soc. A., (1967) 415.
20 Freeman, H.C. and Guss, J.M., Acta Crystallogr. Sect. B, 28 (1972) 2090.
21 Bonnet, J.-J. and Jeannin, Y., Bull. Soc. Fr. Miner. Cristallogr., 93 (1970) 287–299.
22 Bonnet, J.-J. and Jeannin, Y., Bull. Soc. Fr. Miner. Cristallogr., 95 (1972) 61–67.
23 Shvelashvili, A.E., Miminoshvili., E.B., Shchedrin, B.M., Kvitashvili, A.I., Kandelaki, M.N., Sakvarelidze, T.N. and Tavberidze, M.G., Koord. Khim., 6 (1980) 1251.
24 Ahmed, K.J., Habib, A., Haider, S.Z., Malik, K.M.A. and Hess, H.J., Bangladesh Acad. Sci., 4 (1980) 85.
25 Gerber, P.R. and Müller, K., Acta Crystallogr., A43 (1987) 426.
26 Müller, K., Amman, H.J., Doran, D.M., Gerber, P.R., Gubernator, K. and Schrepfer, G., In Van der Goot, H., Domany, G., Pallos, L. and Timmerman, H. (Eds.) Trends in Medical Chemistry, Vol. 88 (Use of Computer Modeling and Structural Databases in Pharmaceutical Research), Elsevier, Amsterdam, 1989, pp. 1-12.
27 Müller, K., Amman, H.J., Doran, D.M., Gerber, P.R., Gubernator, K. and Schrepfer, G., Bull. Soc. Chim. Belg., 97 (1988) 655.
28 Sundberg, R.J. and Martin, R.B., Chem. Rev., 74 (1974) 471.
29 Sigel, H. and Martin, R.B., Chem. Rev., 82 (1982) 385.
30 Bryce, G.F., Roeske, R.W. and Gurd, F.N., J. Biol. Chem., 240 (1965) 3837.
31 Martin, R.B., Chamberlin, M. and Edsall, J.T., J. Am. Chem. Soc., 82 (1960) 495.
32 Freeman, H.C., Guss, J.M. and Sinclair, R.L., J. Chem. Soc. Chem. Commun., (1968) 485.
33 Kim, M.K. and Martell, A.E., J. Am. Chem. Soc., 89 (1967) 5138.
34 Martin, R.B. and Edsall, J.T., J. Am. Chem. Soc., 82 (1960) 1107.
35 Margerum, D.W. and Rosen, H.M., J. Am. Chem. Soc., 89 (1967) 1088.
36 Jones, J.P., Billo, E.J. and Margerum, D.W., J. Am. Chem. Soc., 92 (1970) 1875.
37 Blakeley, R.L., Dixon, N.E. and Zerner, B., Biochim. Biophys. Acta, 744 (1983) 219.
38 Dixon, R.E., Gazzola, C., Asher, C.J., Lee, D.S.W., Blakeley, R.L. and Zerner, B., Can. J. Biochem., 58 (1980) 474.
39 Blakeley, R.L., Webb, E.C. and Zerner, B., Biochemistry, 8 (1969) 1984.
40 Dixon, N.E., Gazzola, C., Blakeley, R.L. and Zerner, B., J. Am. Chem. Soc., 97 (1975) 4131.
41 Williams, R.J.P., J. Mol. Catalysis, Review Issue (1986), pp. 1–27.
42 Hardman, K.D. and Lipscomb, W.N., J. Am. Chem. Soc., 106 (1984) 463.
43 Andrews, R.K., Dexter, A., Blakeley, R.L. and Zerner, B., J. Am. Chem. Soc., 108 (1986) 7124.